

Optical Properties of Er in Er-Doped $\text{Zn}_2\text{Si}_{0.5}\text{Ge}_{0.5}\text{O}_4$ Waveguide Amplifiers

Siddhartha Banerjee, *Student Member, IEEE*, Christopher C. Baker, *Student Member, IEEE*,
Andrew J. Steckl, *Fellow, IEEE*, and David Klotzkin, *Senior Member, IEEE*

Abstract—There is a growing need for compact, efficient integrated waveguide optical amplifiers for use in optoelectronic communication. $\text{Zn}_2\text{Si}_{0.5}\text{Ge}_{0.5}\text{O}_4$ (ZSG) doped with Er (ZSG–Er) is a promising new host material due to the high concentration of Er that can be incorporated and the high optical activity of the incorporated Er. In this paper, the absorption and emission cross sections of Er in ZSG–Er (to the authors' knowledge, for the first time) are measured both through photoluminescence spectra and direct gain and absorption measurements. Peak absorption and emission cross sections are about $3 \times 10^{-24} \text{ m}^2$ from a Landenburg–Fuchtbauer analysis of the photoluminescence spectra, comparable to measurements on other oxide-based glass amplifiers. The population statistics of the excited Er level, along with the excited-state lifetime, are determined through a novel frequency-domain method in which the spontaneous emission power at 1550 nm is measured as a function of frequency under a modulated 980-nm input. The determined lifetime of 2 ms is comparable to the 2.3 ms measured using a conventional pump–probe technique. The novel analysis technique yields the population statistics of the excited Er atoms and the lifetime of the excited Er state under given pumping conditions independent of the unknown and variable coupling in and out of the waveguide. This method predicts zero net gain at 70 mW, about what is observed. Comparison of calculated gain and absorption based on Er density and measured cross sections with measured gains suggest that only about 20%–30% of the Er in the material is optically active. A 4.7-cm-long sample demonstrated a signal enhancement of ~ 13 dB. Cavity characteristics were measured using an analysis of coherent reflection under no pumping. The facet reflectivity was determined to be 0.27, and the scattering/absorption loss was 1.05/cm, for a total distributed loss of 1.65/cm in a 4-cm cavity. These losses, compared with an estimated achievable gain of 0.25/cm under full inversion, suggest that optically pumped lasing at this concentration is not possible. Measurements of both the cross sections and population statistics, compared with actual gain and absorption properties, give insight into the contribution of the Er dopant under different conditions and can be used to model and improve rare-earth-based amplifiers.

Index Terms—Erbium, optical amplifiers, waveguide amplifiers, waveguide components.

I. INTRODUCTION

EFFICIENT integrated optical waveguide amplifiers are important components for optical communication networks. Planar waveguide amplifiers [1]–[3] amplify the signal level in the optical domain and can be easily integrated with other components like modulators [4], multiplexers, and receivers. These optically pumped amplifiers are made with erbium-doped [5],

[6] chalcogenide and oxide glasses [7], [8]. $\text{Zn}_2\text{Si}_{0.5}\text{Ge}_{0.5}\text{O}_4$ (ZSG) doped with Er (ZSG–Er) is a promising new host material [9]–[11] due to the high concentration of Er that can be incorporated and the high optical activity of the incorporated Er. This material has demonstrated 1.5- μm signal enhancement of > 13 dB in a 4.7-cm fabricated ridge waveguide and scattering losses as low as 2.4 dB/cm.

Although the basic amplification mechanism for all of these glass-based amplifiers is the same, the properties of Er vary significantly from host to host. To model, design, and optimize these amplifiers and to improve the performance of Er in each host, it is essential to understand the properties of the Er in the host material [3], [12]. Understanding the interactions between the Er and its host material is critical in optimizing the optically pumped amplifiers and achieving the highest possible amplification.

In this paper, the absorption and emission cross sections of Er in ZSG doped with 0.1 atomic % Er are first determined through analysis of the photoluminescence spectra (to the authors' knowledge, the first measurements of Er cross sections in this host). A novel rate-equation-based analysis, combined with measurement of the spontaneous emission power as a function of both input pump power and pump power modulation frequency, is used to measure the fraction of excited Er and the Er excited lifetime under given pumping conditions. From the measured population statistics and absorption/emission cross section, calculated gain and absorption for given pumping conditions are compared with directly measured gain and absorption. This comparison indicates the fraction of the included Er that is optically active. Although the measured cross sections of Er in ZSG–Er ($\sim 3 \times 10^{-24} \text{ m}^2$) are quite comparable to good values in glass amplifiers [7], [8], [13]–[16], comparison of measured gain with gain calculated with measured cross sections and the known Er concentrations and population statistics clearly showed that the much of the Er in this material was not optically active. The potential gain of ZSG–Er could be much higher with an increase in the optically active fraction. The excited-state lifetime obtained with this technique agrees well with measurements made using a conventional pump–probe technique [17], [18], and in addition the transparency point seen with this technique compared well to that seen in a direct fiber-to-fiber measurement [9], [10].

This can distinguish the effects of cross section (a property of the optically active Er) from the fraction of optically active Er in the device, which a simple gain measurement or cross-section measurements cannot. By systematic study of cross sections, Er lifetime, and fraction of optically active Er as a function of Er

Manuscript received May 5, 2004.

The authors are with the University of Cincinnati, Cincinnati, OH 45221-0030 USA (e-mail: David.Klotzkin@uc.edu).

Digital Object Identifier 10.1109/JLT.2004.839966

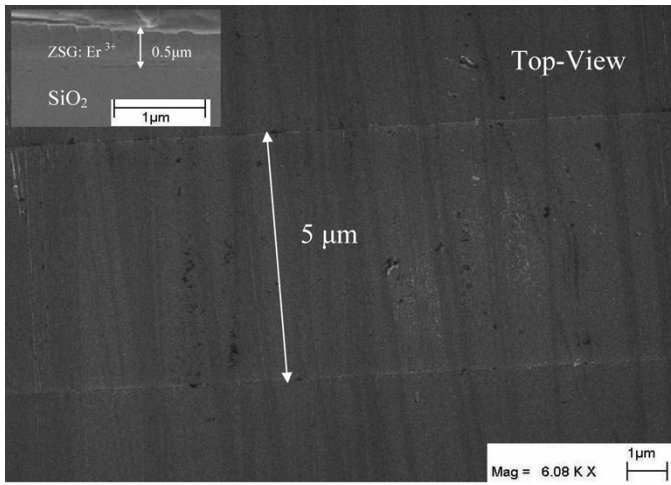


Fig. 1. SEM photomicrograph of a single ZSG waveguide; inset shows the facet of the waveguide.

density, the mechanisms for gain quenching with concentration can be studied.

The actual power that can be coupled out of the device depends also on the cavity scattering and absorption loss and facet quality. The facet reflectivity and absorption/scattering losses of fabricated ridge-waveguide amplifiers made of ZSG–Er on Si substrates was characterized through a simple coherent reflection technique.

II. DEVICE FABRICATION

The ZSG waveguide amplifiers were fabricated at the Nanoelectronics Laboratory of the University of Cincinnati, Cincinnati, OH. A detailed description of the fabrication process can be found in references [9] and [10]. A thin film from a nominally 99.9% $\text{Zn}_2\text{Si}_{0.5}\text{Ge}_{0.5}\text{O}_4\text{--Er}_{0.05}$ target was sputter-deposited at room temperature using a Denton Discovery 18 sputtering system on a 2.5- μm thermal oxide which acts as the lower cladding to the waveguides. After sputtering, the ZSG–Er ridge waveguides were fabricated by Cl–Ar-based inductively coupled plasma (ICP) etching using a Plasmatherm 790 plasma reactor operated in the ICP mode. The waveguides are typically 3–10 μm wide and about 1 μm thick with very shallow etch depths (< 100 nm). After etching, the amplifiers were fabricated either by scribing and cleaving the underlying Si or polishing the exposed facets.

Fig. 1 shows a top view of a scanning electron microscope (SEM) photomicrograph of a single completed ZSG waveguide, with the inset showing a cleaved facet of the same. The wavelength dependence of the refractive indexes of the ZSG film was determined using prism coupling and variable wavelength spectroscopic ellipsometry [9], [10] and was found to be 1.74 at 1.5 μm . Full-wave simulations shows single-mode operation of a 3- μm -wide waveguide with an optical confinement factor (Γ_{opt}) of the 1.5- μm optical mode to the ZSG–Er region of 0.9. Fig. 2 shows the graphical result of such a simulation, showing the modal intensity across the cross section of the waveguide.

The sputtered films were characterized by Rutherford backscattering (RBS) to measure the relative concentrations of the atoms in the fabricated film. The uncertainty in the

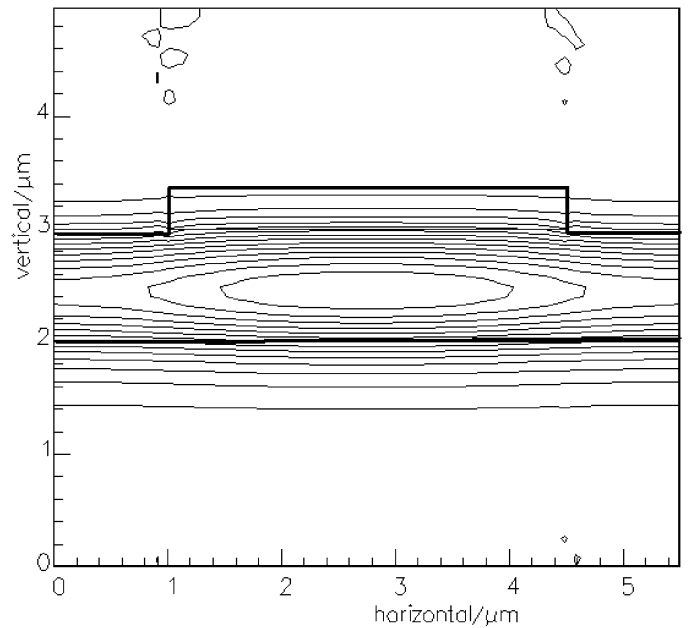


Fig. 2. Full-wave simulation result showing single-mode 3- μm -wide waveguide at a wavelength of 1.55 μm . The optical confinement to the ZSG–Er area is > 0.90 .

measurement was within 5% for O, 2% for Zn, and 1% for Si and Ge. The results showed a stoichiometric ratio of $\text{Zn}_{1.6}\text{Si}_{0.6}\text{Ge}_{0.5}\text{O}_{3.4}$, a significant deviation from its nominal composition. The peak erbium concentration in the ZSG–Er film as found by the RBS technique is $5.88 \times 10^{25} \text{ m}^{-3}$, about 0.1 atomic %.

III. EXPERIMENTAL MEASUREMENT OF CROSS SECTIONS AND LOSS

In order to obtain the emission spectra of Er^{3+} in ZSG, light from a 980-nm pump laser was launched into the cleaved waveguide cavity through one arm of a 2×1 980-nm/1550-nm coupler–combiner to excite the Er^{3+} . The bare cleaved fiber of the combined end was directly coupled to the waveguide, and the reflected signal at 1550 nm was collected after being transmitted back through the splitter and then through the 1550 arm of the coupler to an Ando 6715 optical spectrum analyzer (OSA), where it is recorded.

The magnitude and wavelength dependence of the cross sections are extremely important for predicting the maximum achievable gain of the amplifier at any given level of inversion. The emission cross-section spectrum is derived directly from the photoluminescence spectra of the ZSG–Er waveguides using the Ladenburg–Fuchtbauer equation [15], as follows:

$$\sigma_e(\lambda) = \frac{\lambda_{\text{em}}^2 \lambda^2}{8\pi n^2 c \tau_{10}} \frac{I_{\text{em}}(\lambda)}{\int I_{\text{em}}(\lambda) d\lambda} \quad (1)$$

where n is the refractive index of ZSG ($n = 1.74$), and τ_{10} is the radiative lifetime of the ${}^4I_{13/2}$ state (measured to be 2 ms, as will be discussed hereafter). I_{em} is the emission spectrum, and λ_{em} is the peak wavelength (1534 nm). Fig. 3 shows the emission cross-section spectra from 1500 to 1565 nm. The peak emission cross section, $\sigma_{e,\text{peak}}$ was $3 \times 10^{-24} \text{ m}^2$ at $\lambda =$

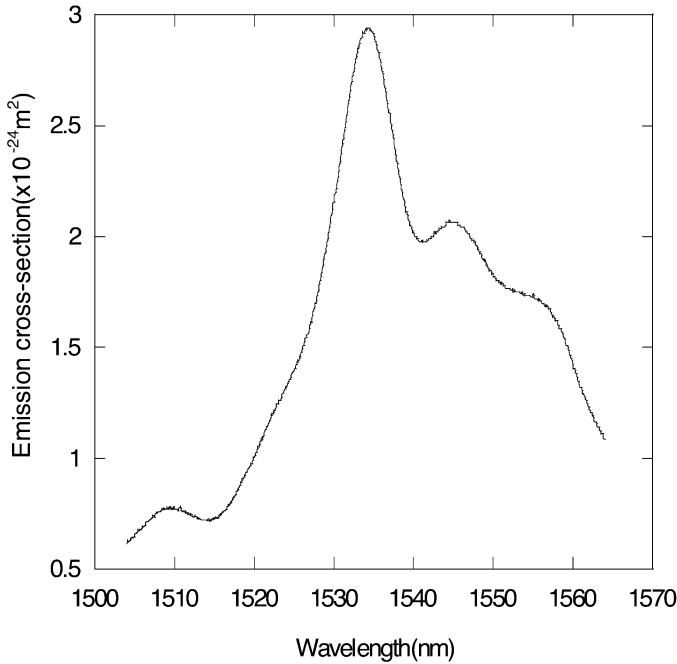


Fig. 3. Emission cross section of ZSG amplifiers (from 1505 to 1565 nm).

1534 nm. The absorption cross-section spectrum $\sigma_a(\lambda)$ was determined from the emission cross-section spectrum $\sigma_e(\lambda)$, using the McCumber relation [14], [20], [21], as follows:

$$\sigma_a(\lambda) = \sigma_e(\lambda) \frac{g_u}{g_l} \exp \left[-\frac{(E_{ZL} - \frac{hc}{\lambda})}{kT} \right] \quad (2)$$

where g_u and g_l are the multiplicities of the ${}^4I_{13/2}$ and ${}^4I_{15/2}$ levels, respectively ($g_u = 7$ and $g_l = 8$), E_{ZL} (zero-level energy) is the energy separation between the lowest levels of each manifold, k is the Boltzman constant, and T the temperature in K .

For direct measurement of both gain and absorption, one fiber was coupled to each facet of a waveguide amplifier. To measure the absorption spectra, light from a tunable laser (with a wavelength range from 1480 to 1570 nm) was launched into the waveguide through the input fiber, and the transmitted light intensity through the output fiber was recorded using a sensitive optical detector. (The waveguide is not pumped during this measurement.) The absorption spectrum was obtained from this transmitted spectrum after corrections for wavelength dependence of the tunable laser output power and other components. The general relationship between output and input power is

$$P_{\text{out}}(\lambda) = x^2 P_{\text{in}}(\lambda) e^{Lg} \quad (3)$$

with g_{net} being the total gain (or loss) experienced in cm^{-1} ; absorption and emission cross section $\sigma_a(\lambda)$ and $\sigma_e(\lambda)$, respectively; and $N_{\text{Er-g}}$ and $N_{\text{Er-x}}$ indicating the number of Er atoms in the ground ($I_{15/2}$) and excited ($I_{13/2}$) state, respectively. The symbol x is the coupling coefficient (~ 0.2) at the fiber-waveguide interface, and L is the length of waveguide

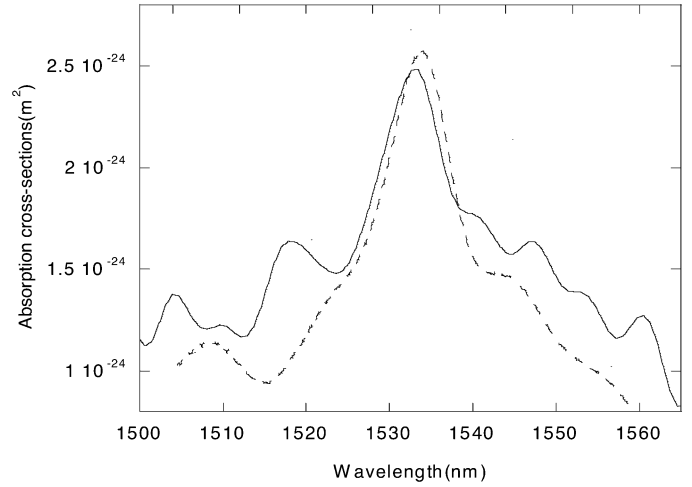


Fig. 4. Absorption cross-section spectrum of ZSG-Er waveguides: directly measured (solid line) and using the McCumber equation (dotted line).

cavity (0.6 cm). For this unpumped absorption measurement, $N_{\text{Er-x}} = 0$. The coupling is estimated by taking the highest ratio of $P_{\text{out}}/P_{\text{in}}$ at wavelengths at which we expect minimal absorption in the waveguide, that is, where the absorption cross section is 0, and estimating x^2 from that. This is a particularly reasonable assumption given our short cavity.

At the peak absorption wavelength of 1534 nm, $P_{\text{out}}/P_{\text{in}} = 0.775$, which implies a absorption cross section of about $1 \times 10^{-24} \text{ m}^2$, or a factor of about 2.5 less than seen through the McCumber analysis of the photoluminescence spectra, if $N_{\text{Er-g}}$ is taken to be an as-fabricated $6 \times 10^{25}/\text{m}^3$. If the cross section is assumed to be correct, the concentration of optically active Er in the waveguides is about 30% of the total concentration.

Fig. 4 shows a plot of the absorption cross-section spectrum made from direct absorption measurements with N_{Er} taken to be $2 \times 10^{25}/\text{m}^3$ and also calculated indirectly using the McCumber theory [14], [20]. With this “fit” value for the number of optically active Er, the peak value of the absorption cross sections agree, and the shape of the curves are in reasonable agreement throughout the spectrum. The peak value of the absorption cross section was $\sigma_{a,\text{peak}} = 2.5 \times 10^{-24} \text{ m}^2$ at 1534 nm.

To characterize the facet reflectivity and internal loss of the cavity, a 1.85-cm-long waveguide cavity was made by cleaving opposite ends of a longer waveguide. The cavity is then characterized as a lossy Fabry-Pérot (F-P) etalon [22], [23]. Light from the tunable laser is fed into this cavity through one arm of a single window 2×1 splitter using end-on coupling, and back-reflected light is picked up using the same fiber and transported through the splitter’s other arm to the optical power meter. An isolator is included between the splitter and the tunable laser to eliminate harmful back reflections that can destabilize the laser output. The tunable laser wavelength is varied from 1540 to 1541 nm in steps of 0.01 nm, and the reflected power spectrum is recorded at each wavelength. This measurement is shown in Fig. 5, along with the best-fit curve. A periodic fluctuation in received optical power was observed due to coherent interference between the reflected light from the front- and back-facet reflected waves and can be well modeled using the lossy F-P

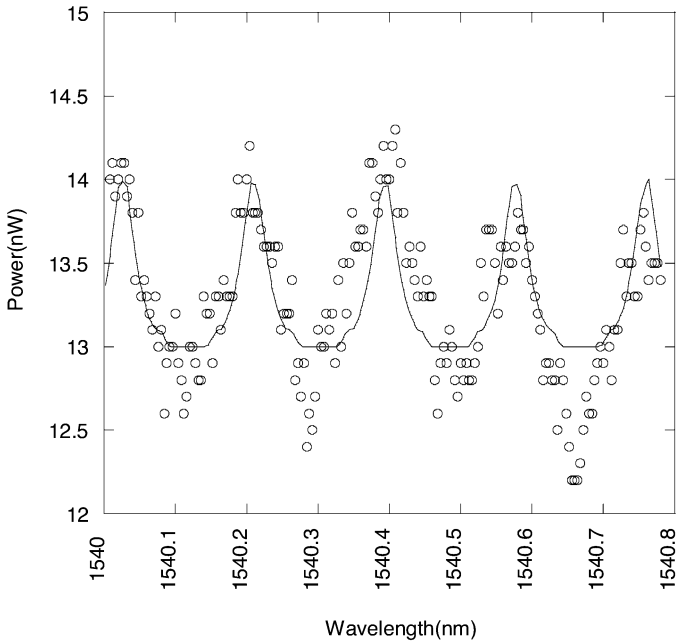


Fig. 5. Measured (dots) and fitted (line) plots for reflected power versus wavelength, demonstrating coherent interference between front and back facet from which reflectivity and absorption could be extracted.

etalon model [22], [23]. The irradiation equation for the reflected wave is

$$\frac{I_{\text{refl}}}{I_{\text{in}}} = \frac{r + re^{-4Ln\alpha} - 2re^{-2Ln\alpha} \cos\left(\frac{4\pi Ln}{\lambda}\right)}{1 + r^2e^{-4Ln\alpha} - 2re^{-2Ln\alpha} \cos\left(\frac{4\pi Ln}{\lambda}\right)} \quad (4)$$

where α is the absorption coefficient (cm^{-1}) of the cavity, r is the reflectance of the facets, L is the length of the cavity (1.85 cm), and n is the refractive index of the core ($n = 1.74$). The obtained spectrum is now fitted to the above equation with reflectance (r) and loss coefficient (α) as fit parameters. Best fit is obtained for $\alpha = 1.05/\text{cm}$ and $r = 0.27$.

While this does involve fitting to a complex curve, with a degree of variability in assigning best-fit values to each of the parameters, the setup is particularly simple, involving just coupling a fiber through a splitter to the waveguide facet, and a remarkable amount of information can be obtained. Measurements reported using the outscattering technique [9], [10] (in which the loss was measured by photographing scattered light from the top of the cavity and assuming the scattered light was proportional to the light in the cavity) yielded a total optical loss $\alpha_{\text{total}} = 2.4 \text{ dB/cm} = 1.7/\text{cm}$ (which includes the scattering and absorption losses), which is of the same order as our obtained result.

The maximum theoretical absorption loss (from the absorption cross section and previously estimated optically active Er fraction) $\alpha_{\text{abs}} = 0.3/\text{cm}$ (completely unpumped). The waveguide scattering loss, therefore, is given by $\alpha_{\text{scattering}} = \alpha_{\text{total}} - \alpha_{\text{abs}}$, or in the range of 1.4–0.8/cm. To overcome this scattering loss with the Er population fully inverted would require an optically active Er concentration of $> 5 \times 10^{25}/\text{m}^3$, about five times larger than the current amount of active Er. Hence, optically pumped lasing is currently not possible but may be with an increase in Er concentration of the

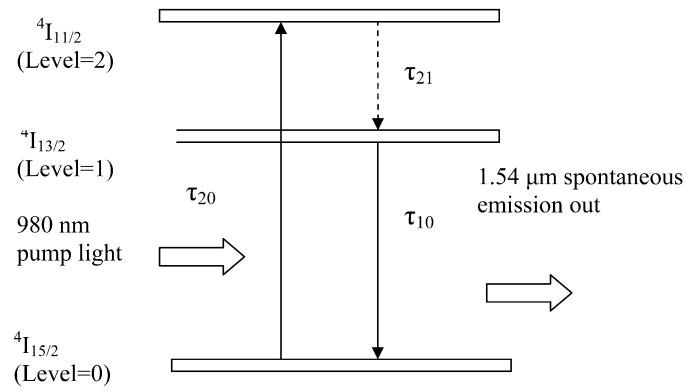


Fig. 6. Model of Er energy levels with relaxation time constants indicating the process of optical pumping and relaxation.

order of five or potentially dramatically reduced waveguide or scattering losses. (In addition to waveguide losses, the cavity chosen would have to be long enough to minimize mirror losses or be facet coated to be very highly reflective.)

IV. MODELING OF CAVITY Er STATISTICS AND Er LIFETIME

With the cross sections known from the photoluminescence spectra, the net gain can be calculated if the Er population statistics (fraction of Er atoms in the excited state $I_{13/2}$ and ground state $I_{15/2}$) are known. The net gain g then experienced is given in (3). However, it is very difficult to measure the population statistics directly. While the pump laser can be set at a certain output, the power coupled into the waveguide amplifier varies and is typically not precisely known.

A careful analysis of the spontaneous emission power with a three-level rate equation model for three Er levels shows that both the population statistics and the Er excited-state lifetime (which is also needed to determine cross sections) can be measured from the analysis of the spontaneous emission power at $1.54 \mu\text{m}$ as a function of both 980-nm pump power and pump modulation frequency. Fig. 6 shows a model of the three-level Er system, as well as the processes used to pump it to achieve amplification. Absorption of a 980-nm photon puts an electron up to the $I_{11/2}$ level, where it rapidly relaxes down to the $I_{13/2}$ level. The metastable $I_{13/2}$ manifold has a lifetime of a few milliseconds (its precise number can be measured, as described) and when it relaxes radiatively, a 1540-nm photon is emitted. The time constants between the levels are shown in the figure.

The rate equations that model [11], [19] the absorption of light by the Er atom, and the relaxation of the Er atom from one state to another, are given as

$$\frac{dI_{15/2}}{dt} = -API_{15/2} + \frac{I_{11/2}}{\tau_{20}} + \frac{I_{13/2}}{\tau_{10}} \quad (5a)$$

$$\frac{dI_{13/2}}{dt} = \frac{I_{11/2}}{\tau_{21}} - \frac{I_{13/2}}{\tau_{10}} \quad (5b)$$

$$\frac{dI_{11/2}}{dt} = API_{15/2} + \frac{I_{11/2}}{\tau_{21}} - \frac{I_{11/2}}{\tau_{20}} \quad (5c)$$

where I_x represents the fractional population of Er atoms in the x state. τ_{10} , τ_{21} and τ_{20} are the characteristic lifetimes of the $I_{13/2} \rightarrow I_{15/2}$, $I_{11/2} \rightarrow I_{13/2}$, and $I_{11/2} \rightarrow I_{15/2}$ transitions, respectively. A is a proportionality constant related to

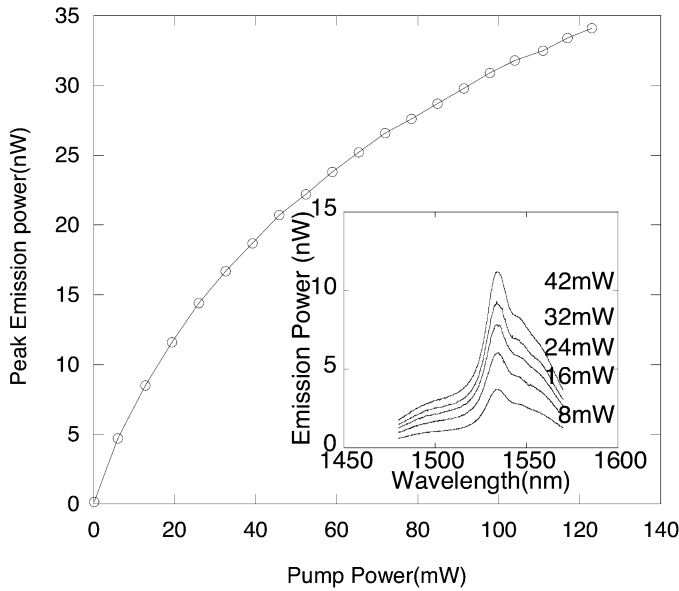


Fig. 7. Plot of the measured (°) and fitted (—) peak spontaneous emission power versus pump power of the 1.85-cm-long ZSG–Er amplifiers. Insert shows typical set of photoluminescence spectra at various pump power levels (for an amplifier of length 0.6 cm).

the coupling and absorption cross section at 980 nm, and P is the pump power. For a constant pump power, the levels are in steady state with the left-hand side of each equation equal to 0; under these conditions, the measured spontaneous emission power $I_{13/2}/\tau_{10}$ is equal to [11]

$$\frac{I_{13/2}}{\tau_{10}} \alpha \frac{m^2 AP}{1 + mAP} \alpha \frac{aP}{1 + bP} \quad (6)$$

where m is the coupling coefficient for both pump power in and spontaneous power out, and a and b are fit parameters. Here, we have neglected the effects of facet reflection and spatial population inhomogeneity, and obtained an “average” population density of the entire cavity.

With this model in mind, the peak spontaneous emission power at $1.53 \mu\text{m}$ was measured as a function of the pump power for a 1.85-cm-long sample and is shown in Fig. 7, along with a best-fit curve. The insert shows a typical data set of photoluminescence spectra taken at several different power levels. The observed roll-off is well modeled by the rate-equation model as given in (6).

Fitting the measured roll-off to the obtained equation allows the populations of the Er atoms to be determined as function of pump power, which allows the expected gain to be calculated. The population inversion of Er can be estimated without an exact knowledge of coupling coefficient. With an estimated coupling of 5%, b can be related to $\sigma_a(980 \text{ nm})$ and is estimated to be about $1\text{--}2 \times 10^{-24} \text{ m}^2$. Since $I_{13/2} = 1 - I_{15/2}$ (due to the very rapid relaxation from the $I_{11/2}$ state), the population densities ($I_{15/2}$ and $I_{13/2}$) can be calculated as a function of pump power for the same 1.85-cm sample, as shown in Fig. 8. Using both measured population statistics and absorption and emission cross sections, the gain per centimeter can be calculated as $g = N_{\text{Er}}(I_{13/2}\sigma_e - I_{15/2}\sigma_a)$, with N_{Er} the density of optically active Er atoms.

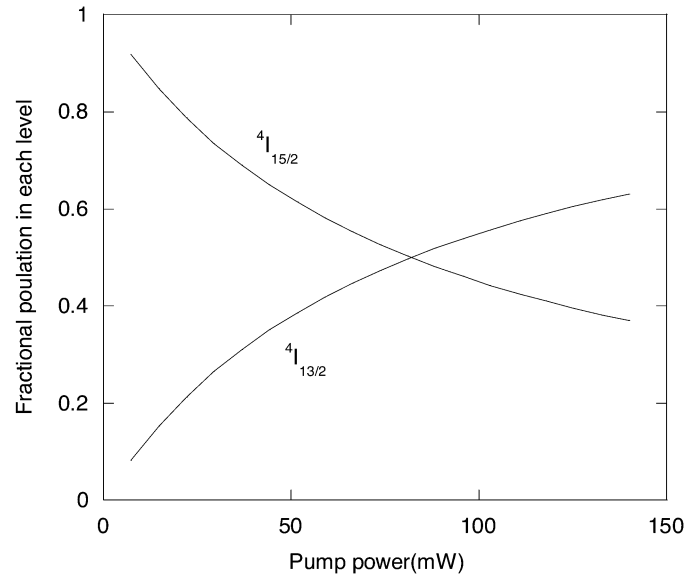


Fig. 8. Fractional populations of the ${}^4I_{13/2}$ and ${}^4I_{15/2}$ levels for different pump powers.

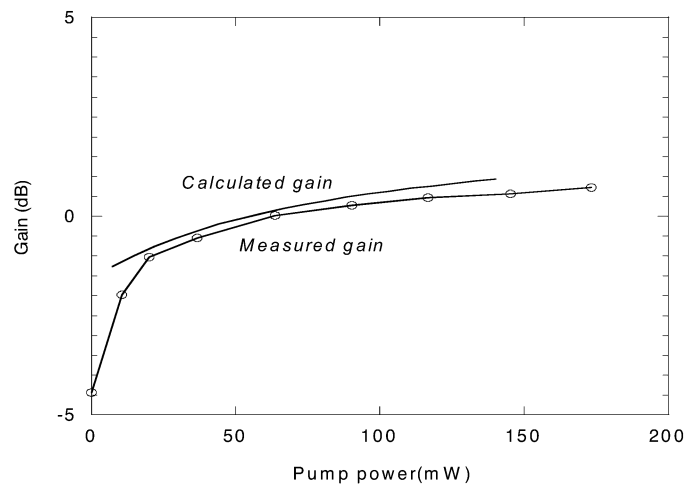


Fig. 9. Calculated and measured gains of a 1.85-cm ZSG–Er amplifier.

Fig. 9 shows the total gain for a 1.85-cm sample compared with the actual gain determined from an available measured 4.7-cm sample (appropriately scaled to 1.85 cm, assuming a uniform gain/unit length). Good agreement with the measured gain was obtained with N_{Er} set to $10^{25}/\text{m}^3$. This is approximately 0.02 atomic %, which is less than the 0.09% nominal Er density (using RBS measurement). Both the values and the transparency point were reasonably well predicted. Similar to the absorption case, only about 20% of the total Er density was active in providing optical gain. In this simple model, we neglect spatial inhomogeneity inside the cavity, the 0.9 confinement factor of the light to the gain region, and potential nonradiative relaxation paths from the excited ($I_{13/2}$) to the ground state ($I_{15/2}$). These factors may also contribute to the discrepancy between measured and expected gain. This model and values of cross section predict a maximum achievable gain in this material of about 0.3 /cm when completely inverted, considering 20% of the Er atoms to be optically active.

This technique can also be extended to provide a simple technique to measure τ_{10} , the lifetime of the Er in the excited $I_{13/2}$ state. A physical setup similar to that of the emission spectrum experiment is used, with the pump laser modulated by a small ac signal superimposed on the dc power. The driving term in the rate equations P is replaced by $P = P_0 + p_1 e^{j\omega t}$, as are the other output terms, as follows:

$$P = P_0 + p e^{j\omega t} \quad (7a)$$

$$I_{13/2} = I_{13/2,0} + i_{13/2} e^{j\omega t} \quad (7b)$$

$$I_{15/2} = I_{15/2,0} + i_{15/2} e^{j\omega t} \quad (7c)$$

$$I_{11/2} = I_{11/2,0} + i_{11/2} e^{j\omega t} \quad (7d)$$

where X represents the total variable, X_0 is the dc component, and x is the time-varying component. The rate equations are solved by combining (7) into (5) and solving for the response of time-varying spontaneous emitted power divided by pump power. Using the rate-equation values and including the steady-state solution, the small-signal response of emitted $1.55\text{-}\mu\text{m}$ power/modulation power $i_{13/2}/\tau_{10}/p$ is given by

$$\frac{i_{13/2}}{p\tau_{10}} = \frac{1}{1 + j\omega\tau_{\text{eff}}} \quad (8)$$

where

$$\tau_{\text{eff}} = \frac{\tau_{10}}{1 + aP_0\tau_{10}} \quad (9)$$

making the reasonable simplifying assumption that $\tau_{21} \ll \tau_{20}$ and τ_{10} . Qualitatively, this assumption can be explained by the relatively long lifetime of the Er $I_{13/2}$ level; at high modulation frequencies of the input power, the slowly changing population of $I_{13/2}$ can not keep pace with the rapid modulation of pump power. The dependence on P_0 of τ_{eff} has to do with the reduced “effective” modulation as the dc population of ground state $I_{15/2}$ reduces with higher pump power.

To measure τ_{10} experimentally, the modulated peak spontaneous emission signal is recorded using the OSA as a tunable filter, centered at the peak wavelength 1534 nm. The analog output of the OSA is used as an input to the Princeton electronics lock-in amplifier locked to the modulating frequency. Using this lock-in technique, modulations in the output power can be clearly seen; the amplitude of the modulated output is measured as a function of frequency and fit to (8) to obtain a value of τ_{eff} . Measurements and fits with two different pump power P_0 levels gave a value for τ_{10} .

Fig. 10 shows the measured and fitted plots for the decrease in signal power with modulation frequency for two different pump power inputs. Best fit is obtained for $\tau_{\text{eff}} = 1.42$ and 1.87 ms for pump powers of 10 and 40 mW, respectively. Finally, the Er $^4I_{13/2}$ lifetime (τ_{10}) is determined using (9) from the two different effective lifetimes to be 1.98 ms, very close to the value reported using time-resolved photoluminescence of 2.3 ms [17], [18].

V. RESULTS AND DISCUSSION

Characterization of the absorption and emission cross section gave cross sections about $2\text{--}3 \times 10^{-24} \text{ m}^2$, typical of what as

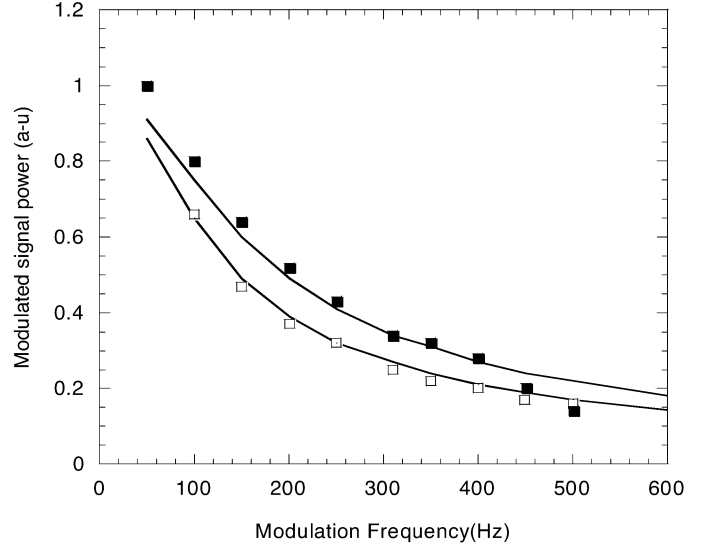


Fig. 10. Variation of modulated signal power at 1534 nm versus frequency for two different pump powers. Dots (\circ) signify actual data points and solid lines (—) are fits.

has been reported in other Er-glass optically pumped amplifiers. Measurement of spontaneous emission power, combined with a novel rate-equation analysis, gave a measurements of Er excited-state lifetime (about 2 ms, consistent with that made using conventional pump–probe techniques) and an estimate of the Er population statistics. These population statistics allow us to compute the expected gain and absorption and compare it directly with the measured gain and absorption.

Comparison for absorption suggests that only 20%–30% of the Er atoms were optically active and participating in resonant absorption. This is a surprisingly large fraction of inert Er and is under investigation. The stoichiometry was sufficiently differently from nominal that different Er atoms could have been in different immediate chemical environments or have been altered from their nominal Er^{3+} state, with potentially reduced activity.

The fraction of Er that contributed to gain was about 20% of the total Er concentration, or about two thirds of that participating in absorption. The fraction of optically active Er is much lower than the as-doped Er fraction, and increasing this fraction would have a dramatic effect on the overall amplifier characteristics. It is possible that optimized sputtering conditions, or incorporating Er via implantation followed by annealing, would increase this proportion. For future study, it would be interesting to measure cross sections and optically active fraction as a function of the concentration to study the mechanisms of concentration quenching and ultimate improve the active fraction of Er in a doped sample.

The method used to determine the Er population statistics and Er excited-state lifetime is quite powerful. Without precise knowledge of the coupling or the use of a pump–probe time-domain technique, both lifetime and pump level can be determined, using a single fiber butt coupled to the facet. The simplicity relies on a lumped model for the Er statistics and does not include spatial inhomogeneity within the cavity. The Er lifetime calculated here from this method of 2 ms agrees quite well with the 2.3 ms measured from a direct pump–probe

method. The power level at which transparency is predicted (with $I_{15/3} = I_{13/2} = 0.5$) obtained through the analysis of spontaneous emission characteristics also agrees well with the measured zero-gain point. These both support the basic validity of this model.

VI. CONCLUSION

ZSG-Er is a very promising new material for optically pumped waveguide amplifiers. The measured cross sections and gain characteristics are quite good, and the measured gain of 2- and 13-dB signal enhancement in a 4-cm-long device is comparable to that of other Er-in-glass waveguide amplifiers [3], [8], [9], [14]. Cavity characteristics as fabricated also show low absorption and scattering loss, indicating the potential for good fiber-to-fiber gain.

The cross sections, measured through analysis of the photoluminescence spectra, are $2\text{--}3 \times 10^{-25} \text{ m}^2$. The Er lifetime and population statistics were determined in a novel way by measurement of the spontaneous emitted power and analysis using a rate-equation-based model and showed good agreement with independently measured Er lifetime and transparency point measurements on fabricated cavity waveguides. This simple and powerful technique agreed well with more direct measurements of the Er lifetime and Er population statistics as a function of pump power.

Analyzed with this technique, the fraction of optically active Er in these structures was determined to be 20%–30%. This factor is significantly impacting the maximum gain obtainable from these devices. It is unclear why such a large fraction of the Er is optically inert, and this is under investigation. It may be due to the Er dopants being in a variety of chemical sites within the glass.

This technique can be also used to study the dynamics of Er in other hosts, and in addition, the change in Er dynamics as a function of concentration in a given host and the mechanism of concentration quenching of the gain.

REFERENCES

- [1] I. Bauman, S. Bosso, R. Brinkmann, R. Corsini, M. Dinand, A. Greiner, K. Schofer, J. Sochtig, W. Sholer, H. Suche, and R. Wessel, "Erbium doped integrated optical devices in LiNbO₃," *IEEE J. Sel. Topics Quantum Electron.*, vol. 2, no. 2, pp. 355–366, Jun. 1996.
- [2] G. N. van den Hoven, J. A. van der Elsken, A. Polman, C. van Dam, J. W. M. van Uffelen, and M. K. Smit, "Absorption and emission cross sections of Er³⁺ in Al₂O₃ planar waveguides," *J. Appl. Opt.*, vol. 36, no. 15, pp. 3338–3341, 1997.
- [3] A. Polman, "Erbium doped planar optical amplifiers," in *10th Eur. Conf. Integrated Optical (ECIO)*, Paderben, Germany, Apr. 2001, pp. 75–79.
- [4] K. Noguchi, O. Mitomi, and H. Miyazawa, "Millimeter-Wave Ti:LiNbO₃ optical modulators," *J. Lightw. Technol.*, vol. 16, no. 4, pp. 615–619, Apr. 1998.
- [5] E. Desurvire, *Erbium Doped Fiber Amplifiers: Principles and Application*, NY: Wiley, 1994.
- [6] B. J. Ainalie, "A review of the fabrication and properties of erbium-doped fibers for optical amplifiers," *J. Lightw. Technol.*, vol. 9, no. 2, pp. 220–238, Feb. 1991.
- [7] S. A. Payne, L. L. Chase, L. K. Smith, W. L. Kway, and W. F. Krupple, "Infrared cross-section measurements for crystals doped with Er³⁺, Tm³⁺, Ho³⁺," *IEEE J. Quantum Electron.*, vol. 28, no. 11, pp. 2619–2630, Nov. 1992.
- [8] D. J. Coleman, S. D. Jackson, P. S. Golding, and T. A. King, "Spectroscopic and energy transfer measurements for Er³⁺-doped and Er³⁺, Pr³⁺-codoped PbO–Bi₂O₃–Ga₂O₃ glasses," *J. Opt. Soc. Amer. B, Opt. Phys.*, vol. 19, pp. 2927–2937, 2002.
- [9] C. C. Baker, J. Heikenfeld, and A. J. Steckl, "Photoluminescent and electroluminescent Zn₂Si_{0.5}Ge_{0.5}O₄: Mn thin films for integrated optic devices," *IEEE J. Sel. Topics Quantum Electron.*, vol. 8, no. 6, pp. 1420–1426, Nov.–Dec. 2002.
- [10] C. C. Baker, J. Heikenfeld, Z. Yu, and A. J. Steckl, "Optical amplification and electroluminescence at 1.54 μm in Er-doped zinc silicate germanate on silicon," *Appl. Phys. Lett.*, vol. 84, no. 9, pp. 1462–1464, Mar. 2004.
- [11] S. Banerjee, C. C. Baker, D. Klotzkin, and A. J. Steckl, "Gain characteristics of Er-doped ZSG waveguide optical amplifiers," in *Proc. IEEE Lasers Electro-Optics Soc. Annu. Meeting*, vol. 1, 2003, pp. 136–137.
- [12] I. V. Voroshilov, V. A. Lebedev, B. V. Ignatiev, A. N. Gavrilenko, V. A. Isaev, and V. F. Pisarenko, "Optical properties of CaGd₄Si₃O₁₃ (CGS) crystals with Er³⁺ used as 1.5 μm laser material," *J. Phys., Condens. Matter*, vol. 12, pp. L287–L292, 2000.
- [13] G. Lifante, E. Cantelar, J. A. Munoz, R. Nevado, J. A. Sanz-Garcia, and F. Cusso, "Zn-diffused LiNbO₃:Er³⁺/Tb³⁺ as a waveguide material," *Opt. Mat.*, vol. 13, pp. 181–186, 1999.
- [14] C. Huang, L. McCaughan, and D. Gill, "Evaluation of absorption and emission cross-sections of ER-doped LiNbO₃ for application to integrated optic amplifiers," *J. Lightw. Technol.*, no. 5, pp. 803–809, May 1994.
- [15] J. A. Lazaro, J. A. Valles, and M. A. Rebolledo, "Determination of emission and absorptions of Er³⁺ in Ti:LiNbO₃ waveguides from transversal fluorescent spectra," *Pure Appl. Opt.*, vol. 7, pp. 1363–1371, 1998.
- [16] C. Strohhofer and A. Polman, "Absorption and emission spectroscopy in Er³⁺-Yb³⁺ doped aluminum oxide waveguides," *Opt. Mat.*, vol. 21, pp. 705–712, 2003.
- [17] R. Wu, J. D. Myers, M. J. Myers, and C. Repp, "Fluorescence lifetimes and 980 nm pump energy transfer dynamics in erbium and ytterbium co-doped phosphate laser glasses," presented at the Photonics West, San Jose, CA, Jan. 28–30, 2003.
- [18] E. E. Nyein, U. Homerich, J. Heikenfeld, D. S. Lee, A. J. Steckl, and J. M. Zavada, "Spectral and time-resolved photoluminescence studies of Eu-doped GaN," *Appl. Phys. Lett.*, vol. 82, no. 11, pp. 1655–1657, Mar. 2003.
- [19] V. Dierolf, A. B. Kutsenko, C. Sandman, F. Tallian, and W. Von der Osten, "Toward new lasers in Ti:Er:LiNbO₃ waveguides: A study of the excited state Er³⁺ states," *J. Appl. Phys. B*, vol. 68, pp. 767–775, 1999.
- [20] D. E. Mc Cumber, "Einstein relations connecting broadband emission and absorption spectra," *Phys. Rev.*, vol. 136, pp. A954–A957, 1964.
- [21] C. Labbe, J. L. Doualan, S. Girard, R. Moncorge, and M. Thuau, "Absolute excited state absorption cross-section measurements in Er³⁺:LiYF₄ for laser application around 2.8 μm and 551 nm," *J. Phys., Condens. Matter*, vol. 12, pp. 6943–6957, 2000.
- [22] S. Yakov, Howe, and G. Dennis, "Some characteristics of an extremely short-external-cavity laser diode realized by butt coupling a Fabry–Pérot laser diode to a single-mode optical fiber (1998)," *J. Appl. Opt.*, vol. 37, no. 15, pp. 3256–3263, 1999.
- [23] H. Haus, *Wave Fields in Opto-Electronics*. Englewood cliffs, NJ: Prentice-Hall, 1984.



Siddhartha Banerjee (S'03) was born in Calcutta, India, on April 19, 1977. He received the B.Sc. (Hons.) degree in physics and the B.Tech. degree in radio-physics and electronics from the University of Calcutta, Calcutta, India, in 1999 and 2002, respectively. He is currently working toward the M.S. degree in electrical engineering with a focus on electronic materials and devices in the Department of Electrical and Computer Engineering and Computer Science at the University of Cincinnati, Cincinnati, OH.

His current research interests include the characterization of erbium-doped waveguide amplifiers for photonic integrated circuits and development of hybrid photonic crystal-conventional waveguide devices.

Mr. Banerjee is a Student Member of Institution of Electrical Engineers (IEE), London, U.K.



Christopher C. Baker (S'00) received the B.S. degree in physics from Miami University, Oxford, OH, in 1998. He received the Ph.D. degree in electrical engineering from the University of Cincinnati, Cincinnati, OH, in 2003, where he focused on active and passive integrated optic components.

In 2001, he joined the Nanoelectronics Laboratory, University of Cincinnati, as a Research Associate to study novel rare-earth-based photonic devices, and in 2003, he joined Intel Corporation, Portland, OR.

Dr. Baker was awarded a scholarship under the Miami University Undergraduate Summer Scholar program for his research in the field of giant magnetoresistance.

Andrew J. Steckl (S'70–M'73–SM'79–F'99) received the B.S.E. degree in electrical engineering from Princeton University, Princeton, NJ, in 1968, and the M.Sc. and Ph.D. degrees from the University of Rochester, Rochester, NY, in 1970 and 1973, respectively.

In 1972, he joined the Honeywell Radiation Center, Lexington, MA, as a Senior Research Engineer, where he worked on new concepts and devices in the area of infrared detection. In 1973, he joined the Technical Staff of the Electronics Research Division of Rockwell International, Anaheim, CA, where he was primarily involved in research on charge-coupled devices. In 1976, he joined the Electrical, Computer and Systems Engineering Department at Rensselaer Polytechnic Institute, Troy, NY, where he developed a research program in microfabrication of Si devices. In 1981, he founded the Center for Integrated Electronics, a multidisciplinary academic center focused on very-large-scale integration research and teaching, and served as its director until 1986. In 1988, he joined the Electrical and Computer Engineering Department of the University of Cincinnati, Cincinnati, OH, as Ohio Eminent Scholar and Gieringer Professor of Solid State Microelectronics. At the university, he has built the Nanoelectronics Laboratory with research in semiconductor materials and devices for photonics. Current activities include GaN molecular beam epitaxy growth, rare-earth-doped luminescent devices, hybrid inorganic/organic materials, and devices for flat panel displays and solid-state lighting. His research has resulted in more than 310 publications and more than 350 conference and seminar presentations.



David Klotzkin (SM'03) received the B.S. degree in electrical engineering from Rensselaer Polytechnic Institute, Troy, NY, in 1988, the M.S. degree in materials science from Cornell University, Ithaca, NY, in 1994, and the M.S. and Ph.D. degrees in electrical engineering from the University of Michigan, in 1997 and 1998, respectively.

His research interests are in optoelectronics devices, including semiconductor lasers, waveguide amplifiers, organic light emitters, and photonic-crystal-based planar lightwave circuits.

His industrial experience includes three years of graphics hardware design at IBM Corporation (1988–1991) and several years of semiconductor laser design for telecommunications applications at various companies, including Lucent Technologies and Agere Systems. In 2002, he joined the Electrical, Computer Engineering and Computer Science Department at the University of Cincinnati, Cincinnati, OH.